

In press as:

Kortsmit J, Davies NH, Miller R, Zilla P, Franz T. Computational Predictions of Improved of Wall Mechanics and Function of the Infarcted Left Ventricle at Early and Late Remodelling Stages: Comparison of Layered and Bulk Hydrogel Injectates. *Advances in Biomechanics and Applications*, 2013.

# Computational Predictions of Improved of Wall Mechanics and Function of the Infarcted Left Ventricle at Early and Late Remodelling Stages: Comparison of Layered and Bulk Hydrogel Injectates

Jeroen Kortsmit<sup>1#</sup>, Neil H. Davies<sup>1</sup>, Renee Miller<sup>1+</sup>, Peter Zilla<sup>1</sup> and Thomas Franz<sup>1-4\*</sup>

<sup>1</sup>*Cardiovascular Research Unit, Chris Barnard Division of Cardiothoracic Surgery, University of*

<sup>2</sup>*Center for Research in Computational and Applied Mechanics, University of Cape Town, Rondebosch, South Africa*

<sup>3</sup>*Research Office, University of Cape Town, Mowbray, South Africa*

<sup>4</sup>*Center for High Performance Computing, Rosebank, South Africa*

(Received , Revised , Accepted )

**Abstract.** Acellular intra-myocardial biomaterial injections have been shown to be therapeutically beneficial in inhibiting ventricular remodelling of myocardial infarction (MI). Based on a biventricular canine cardiac geometry, various finite element models were developed that comprised an ischemic (II) or scarred infarct (SDI) in left ventricular (LV) antero-apical region, without and with intra-myocardial biomaterial injectate in layered (L) and bulk (B) distribution. Changes in myocardial properties and LV geometry were implemented corresponding to infarct stage (tissue softening vs. stiffening, infarct thinning, and cavity dilation) and injectate (infarct thickening). The layered and bulk injectate increased ejection fraction of the infarcted LV by 77% (II+L) and 25% (II+B) at the ischemic stage and by 61% (SDI+L) and 63% (SDI+B) at the remodelling stage. The injectates decreased the mean end-systolic myofibre stress in the infarct by 99% (II+L), 97% (II+B), 70% (SDI+L) and 36% (SDI+B). The bulk injectate was slightly more effective in improving LV function at the remodelling stage whereas the layered injectate was superior in functional improvement at ischemic stage and in reduction of wall stress at ischemic and remodelling stage. These findings may stimulate and guide further research towards tailoring acellular biomaterial injectate therapies for MI.

**Keywords:** myocardial infarct, therapeutic injection, cardiac remodelling, finite element method

---

## 1. Introduction

An estimated 17.3 million people died from cardiovascular diseases in 2008, representing 30% of all global deaths. Of these deaths, approximately 7.3 million were due to ischemic heart disease or myocardial infarction (MI) (Mendis *et al.* 2011). Myocardial infarction is caused by occlusion of a coronary artery leading to a shortage of oxygen and nutrients in a part of the cardiac muscle

\*Corresponding author. Email: thomas.franz@uct.ac.za

# Claude Leon Postdoctoral Fellow

+Whitaker Fellow

(Holmes *et al.* 2005). This results in necrosis of the affected (infarcted) myocardium and a direct loss of contractile properties. Breakdown of the extracellular matrix is initiated which makes the infarcted myocardium more prone to extension and dilation. Stresses in the myocardial wall increase due to these geometrical changes, and the cardiac pump function is negatively influenced. Consequently, a cascade of compensatory mechanisms – post-MI remodelling - is initiated in an attempt to maintain normal cardiac functionality. However, despite its beneficial purpose, this series of biological changes including alterations in extracellular matrix and cell-cell interactions, dilation and hypertrophy of the left ventricle (LV) often progresses into a feedback loop that eventually results in heart failure (Sam *et al.* 2000, Sutton and Sharpe 2000, Holmes *et al.* 2005, Katz 2008, Pilla *et al.* 2009). Different strategies have been adopted to prevent the adverse ventricular remodelling process. Among these, the mechanical approach focuses on the inhibition and reduction of ventricular dilation to maintain or restore cardiac geometry and to limit ventricular wall stresses and thinning (Nelson *et al.* 2011). Cardiac restraint devices and advanced surgical procedures have been utilized in the clinic with varying degrees of success. A potentially less invasive strategy is the injection of biomaterials into the cardiac wall and this has been increasingly investigated over the last decade with improvement of cardiac functionality and reduction of post-MI remodelling having been shown in experimental studies (Christman *et al.* 2004, Landa *et al.* 2008, Ifkovits *et al.* 2010). A wide variety of biomaterials including natural (Dai *et al.* 2005, Landa *et al.* 2008) and synthetic (Dobner *et al.* 2009, Kadner *et al.* 2012) polymers has been tested; exhibiting a broad range of properties including mechanical behaviour, biodegradability, volume, and distribution. While a few experimental studies have begun to study the optimization of certain properties such as stiffness (Ifkovits *et al.* 2010) and bio-degradability (Tous *et al.* 2011) of the injected biomaterial, more research is needed to clarify the specific mechanisms behind functional and mechanical improvements resulting from biomaterial inclusion in a post-MI heart.

Cardiac mechanics and the effects of pathologies, such as myocardial infarct, have been studied with success using finite element (FE) methods (e.g. Moustakidis *et al.* 2002, Beg *et al.* 2004, Walker *et al.* 2005). However, myocardial injectates for MI therapies have not yet received much attention in FE studies. Wall *et al.* (2006) investigated the effect of biomaterial injections into the border zone and infarct regions in a previously validated FE model of an ovine LV with an antero-apical (AA) infarct (Walker *et al.* 2005). A decrease in end-systolic LV stress was found that was proportional to the volume and stiffness of the injected biomaterial. Additionally, the ejection fraction (EF) was slightly better but the stroke volume (SV) divided by LV end diastolic pressure was not increased due to the biomaterial inclusion. Wenk *et al.* (2011) examined the effects of injecting a calcium-hydroxyapatite tissue filler on the passive material response of infarcted left ventricles. A methodology was developed for using 3D echocardiography images from a treated and untreated AA infarct to generate FE models and estimate the material properties in the infarct and remote (healthy) myocardial region. The passive stiffness value in the treated infarct region was found to increase by nearly 345 times the healthy value, and the thickness of the infarct wall was also increased. Overall, akinesia in the infarct was caused by the inclusion of tissue filler

which generally reduced LV stresses. Although these studies have made important progress, further refinements are required to achieve a closer approximation to the *in vivo* scenario. In both studies, the treated infarct was assumed to be homogeneous. No distinctions were made between the properties of the infarcted region and the injected biomaterial. Material properties were defined by applying a volume mixing rule without modelling the distribution of the injected biomaterial and tissue response separately. In the study of Wenk *et al.* (2009), a finite element (FE) based method was developed to optimize the injection pattern of spherical polymeric inclusions in a dilated canine LV at early diastole according to a specific objective function. When only the LV myofibre stress was incorporated in the objective function, a decrease of stresses was shown as the number of inclusions increased. A different outcome was obtained when both stress and stroke volume were considered in the objective function. In that study, the geometry and material properties of the biomaterial and LV myocardial tissue were described independently. However, the shape and distribution of the injected material were not based on experimental work. Furthermore, the infarcted tissue itself was not defined in the model with the diseased state of the heart being represented only by its dilated geometry. The main limitation of these recent FE studies is the simplified fashion in which the biomaterials injected into the myocardium were modelled. Treated infarct regions were assumed homogeneous (Wall *et al.* 2006, Wenk *et al.* 2011), infarcted regions were not defined (Wenk *et al.* 2009) and a micro-structural realistic representation of the distribution of the injected biomaterial was not provided (Wall *et al.* 2006, Wenk *et al.* 2009, Wenk *et al.* 2011).

In our previous study, the definition of the geometrical shape and material properties of the injected biomaterial, infarcted myocardium and healthy tissue were based on experimental studies (Dobner *et al.* 2009, Kadner *et al.* 2012) and modelled separately (Kortsmit *et al.* 2012). In a canine heart FE model, four AA infarct models were created representing different temporal phases in the progression of a myocardial infarction. Hydrogel layers were simulated as multiple thin layers in the infarcted myocardium in each model. Biomechanical and functional improvement of the LV was found after hydrogel inclusion in the ischemic models representing the early phases of myocardial infarction.

The aim of the current study was to expand our recent research and improve the link between numerical and *in vivo* work by considering the overall dilation of the LV associated with post-infarct remodelling and representing both layered and bulk distributions of hydrogel injectates experimentally observed. The objective of this study was to compare the effects that these two characteristic injectate distributions have on cardiac functionality and wall mechanics at an early and late stage after infarction.

## **2. Materials & Methods**

The finite element simulations for large displacement and finite strain utilised a validated canine heart model comprising a left and right ventricular geometry and 3D myofibre angle

distribution (Nielsen *et al.* 1991) in Continuity®6.4 (University of California in San Diego, CA, USA) (Kerckhoffs *et al.* 2007). As described previously (Kortsmit *et al.* 2012), the FE mesh was created from the unloaded, resting healthy heart with cavity volumes of the left and right ventricle of 26.1 and 22.3 ml, respectively. The initial mesh of 48 tricubic Hermite elements in a 4 x 3 x 4 grid (circumferential x longitudinal x transmural) was refined in the transmural direction when required.

## 2.1 Constitutive models

Passive mechanical properties of the myocardium were modelled using a nearly incompressible, transversely isotropic strain energy function  $W$ :

$$W = \frac{1}{2}C(e^Q - 1) + C_{\text{compr}}(\det(\mathbf{F})\ln(\det(\mathbf{F}) - \det(\mathbf{F}) + 1)) \quad (1)$$

with

$$Q = b_{\text{ff}}E_{\text{ff}}^2 + b_{\text{cc}}(E_{\text{cc}}^2 + E_{\text{ss}}^2 + E_{\text{cs}}^2 + E_{\text{sc}}^2) + b_{\text{fc}}(E_{\text{fs}}^2 + E_{\text{sf}}^2 + E_{\text{fc}}^2 + E_{\text{cf}}^2) \quad (2)$$

where  $E_{\text{ff}}$  is the fibre strain,  $E_{\text{cc}}$  is cross-fibre in-plane strain,  $E_{\text{ss}}$  is the radial strain transverse to the fibre,  $E_{\text{cs}}$  is the shear strain in the transverse plane, and  $E_{\text{fc}}$  and  $E_{\text{fs}}$  are shear strain in fibre – cross-fibre and fibre – radial coordinate planes, respectively. The material parameters for healthy passive myocardium were the same as in our previous study (Kortsmit *et al.* 2012):  $C = 0.88$  kPa,  $b_{\text{ff}} = 18.5$ ,  $b_{\text{cc}} = 3.58$  and  $b_{\text{fc}} = 1.63$  were determined previously for healthy canine myocardium (Guccione *et al.* 1991). To enforce the nearly incompressible material behavior of the passive myocardium, the penalty function U8 (Doll and Schweizerhof 2000) was added to the strain energy function  $W$ , Eq. (1), with a bulk modulus of  $C_{\text{compr}} = 100$  kPa (Kortsmit *et al.* 2012).

Stress in the contracting myocardium was derived as the sum of the passive stress (from Eq. (1)) and an active fibre directional stress component  $T_0 = f(t, Ca_0, l_0, l_R, T_{\text{max}})$  with the material parameters  $Ca_0 = 4.35$   $\mu\text{mol/l}$  (peak intra-cellular calcium concentration),  $l_0 = 1.58$   $\mu\text{m}$  (sarcomere length at which no active tension develops),  $l_R = 1.85$   $\mu\text{m}$  (stress-free sarcomere length) and  $T_{\text{max}} = 137.5$  kPa (maximum isometric tension at maximum sarcomere length) (Guccione and McCulloch 1993).

## 2.2 Infarct models

Using the reference model of the healthy heart, two models with an AA infarct were generated representing an early and late stage of infarct healing stage after occlusion of the coronary artery (Table 1). The early healing stage was represented by the ischemic infarct model (II). During the early ischemic infarct stage, the infarcted myocardium is converted from contractile to non-contractile tissue (Holmes *et al.* 2005). Hence, contraction in the AA region of the model was disabled, i.e.  $Ca_0 = 0$   $\mu\text{mol/l}$ . The passive mechanical properties of the infarcted myocardium were decreased, by setting  $C = 0.22$  kPa, to account for necrosis and degradation of structural proteins

(Holmes *et al.* 2005). All other parameters were the same as in the reference model of the healthy heart. In human, the ischemic and necrotic phases in the MI healing process end approximately one week after the onset of an MI, after which the fibrotic phase commences. Scar formation in the infarcted region results in a large increase in tissue stiffness and thinning of the infarcted wall (Holmes *et al.* 2005). These structural changes are mostly accompanied by dilation of the LV cavity. Therefore, this stage was simulated by a model comprising a scarred infarct and dilated LV cavity, in the following referred to as scarred dilated infarct (SDI). The higher stiffness and non-contractility of the scarred infarct were represented by a ten-fold increased stress scaling coefficient  $C = 8.8$  kPa (Sun *et al.* 2009) and  $Ca_0 = 0$   $\mu\text{mol/l}$ , respectively. The thickness of the infarcted wall was reduced from both the endo- and epicardial side corresponding to a volume reduction of 9.4 ml. LV dilation was mimicked by increasing the LV cavity volume by 100% (Pfeffer and Braunwald 1990, Morita *et al.* 2011, Kadner *et al.* 2012) from 26.1 ml (healthy reference model) to 52.2 ml. Other parameters remained as in the healthy heart model (Guccione *et al.* 2001, Dang *et al.* 2004, Dang *et al.* 2005).

Table 1: Specifications of the FE models: Number of elements overall and transmurally, LV cavity volume, LV wall volume, wall volume of the AA region, and volume of the hydrogel injectate.

Model		No of Elements			Volume (ml)		
		Total	Transmural	LV cavity	LV wall	AA wall region	Hydrogel
Healthy Control	H	48	4	26.1	97.4	28.4	-
Ischemic Infarct	II	48	4	26.1	97.4	28.4	-
+ layered injectate	II+L	108	9	24.8	104.3	37.7	9.4
+ bulk injectate	II+B	96	8	24.8	104.3	37.7	9.4
Scarred Dilated Infarct	SDI	48	4	53.2	97.8	23.2	-
+ layered injectate	SDI+L	144	12	45.9	103.2	32.6	9.4
+ bulk injectate	SDI+B	96	8	45.9	103.2	32.6	9.4

### 2.3 Hydrogel injectates

Two different biomaterial distributions in the infarct were simulated; a layered and a bulk configuration (Fig. 1). The layered hydrogel inclusion was described by alternating thin layers centred in the infarct region, approximating the multi-layered distribution observed *in vivo* (Dobner *et al.* 2009, Kadner *et al.* 2012). The bulk injectate consisted of one thick layer incorporated in the centre of the infarct (Landa *et al.* 2008, Morita *et al.* 2011, Kadner *et al.* 2012). For both distributions, the total volume of the hydrogel was 9.4 ml representing 7% of the total wall volume. The injectate volume was added to the volume of infarcted region leading to wall thickening. The thickness of the infarcted wall was increased from both the endo- and epicardial side in all infarct models with injectate.

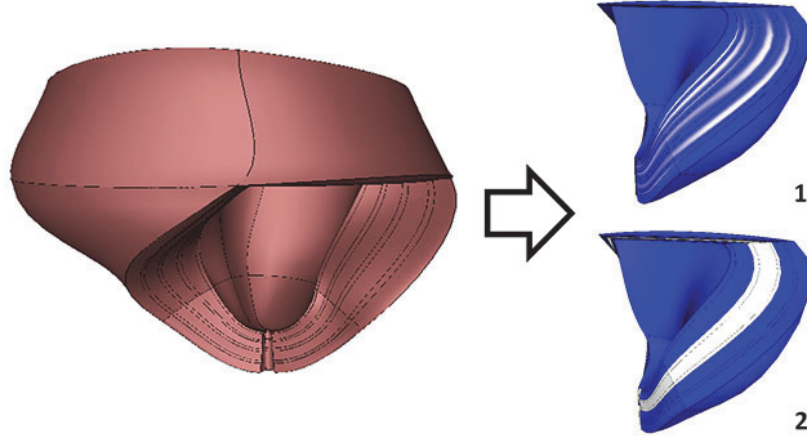


Fig. 1 Three-dimensional biventricular finite element model of a canine heart (with infarcted antero-apical region removed for illustration purposes) illustrating (1) the layered hydrogel injectate and (2) the bulk injectate infarcted wall in one of the infarct models. (Colour code: brown – healthy tissue, blue – infarcted tissue, white – hydrogel)

Mechanical properties of the isotropic hydrogel were modelled by choosing the same value, 18.5, for the strain and shear coefficients  $b_{ff}$ ,  $b_{cc}$  and  $b_{fc}$ , in the strain energy function, Eq. (1). The stiffness of the hydrogel was based on a non-degradable polyethylene glycol (PEG) hydrogel used in an *in vivo* study (Dobner *et al.* 2009). Experimental tests indicated the stiffness of the PEG gel to be 50% of that of healthy myocardium (unpublished results), hence for the hydrogel  $C = 0.44$  kPa was employed.  $Ca_0 = 0$   $\mu\text{mol/l}$  accounted for non-contractility.

#### 2.4 Cardiac haemodynamics

Measures for LV cardiac haemodynamics used were; end-systolic (ESPVR) and end-diastolic pressure-volume relationships (EDPVR), end-systolic elastance, or contractility, ( $E_{ES}$ ), and dead space volume ( $V_0$ ).  $E_{ES}$  and  $V_0$  are obtained from slope and volume intercept of the ESPVR curve, respectively. The LV functional parameters stroke volume (SV) and ejection fraction (EF) were calculated by

$$SV = V_{ED} - V_{ES} \quad (3)$$

and

$$EF = \frac{SV}{V_{ED}} \quad (4)$$

with  $V_{ED}$  and  $V_{ES}$  being end-diastolic and end-systolic ventricular volume determined at the associated pressure of 1.33 kPa (10 mmHg) and 13.3 kPa (100 mmHg), respectively.

## 2.5 Myocardial mechanics

Mid-wall LV and mean infarct myofibre stresses in reference to the local myofibre orientation were calculated for the healthy control and the infarct models. For all cardiac models, mean infarct fibre stress values were obtained at the Gaussian points of each element and the average value per element was weighted by the element volume. Stress values were obtained and averaged at end-diastole ( $P = 10 \text{ mmHg} = 1.33 \text{ kPa}$ ) and end-systole ( $P = 100 \text{ mmHg} = 13.33 \text{ kPa}$ ).

## 3. Results

### 3.1 Cardiac function

The haemodynamics predicted with the different cardiac models are represented as end-diastolic and end-systolic pressure-volume (PV) relationships of each model from which the cardiac functional parameters were calculated, see Table 2. ESPVR and EDPVR for all models are shown in Fig. 2.

#### 3.1.1 Infarct models

In the PV loops of the two infarct models without hydrogel injectate (Fig. 2a), a clear shift to the right of the ESPVR curves compared to the healthy reference case is observed. This rightward shift is largest for the SDI model. For the EDPVR, a similar rightward shift is seen for the SDI case while no difference is observed between the ischemic infarct (II) case and the healthy (H) case. With regard to the cardiac function, a decrease in contractility  $E_{ES}$  of 19% and 54% relative to the healthy reference is shown for models II and SDI. An increase in  $V_0$  by 63% and 183%, a reduction of SV of 70% and 39%, and a drop in EF of 71% and 67% are seen for II and SDI cases, respectively, in comparison to the healthy control case (Table 2).

Table 2 Results of cardiac function represented by contractility  $E_{ES}$ , dead space volume  $V_0$ , stroke volume SV and ejection fraction EF for the different cardiac models.

Model		Cardiac functional parameters			
		$E_{ES}$ (kPa/ml)	$V_0$ (ml)	SV (ml)	EF (%)
Healthy Control	H	0.979	13.9	15.2	35.6
Ischemic Infarct	II	0.794	22.7	4.58	10.4
+ layered injectate	II+L	0.806	17.0	7.55	18.4
+ bulk injectate	II+B	0.919	20.3	5.17	13.0
Scarred Dilated Infarct	SDI	0.449	39.4	9.28	11.8
+ layered injectate	SDI+L	0.483	27.9	13.0	19.0
+ bulk injectate	SDI+B	0.468	27.2	13.2	19.2

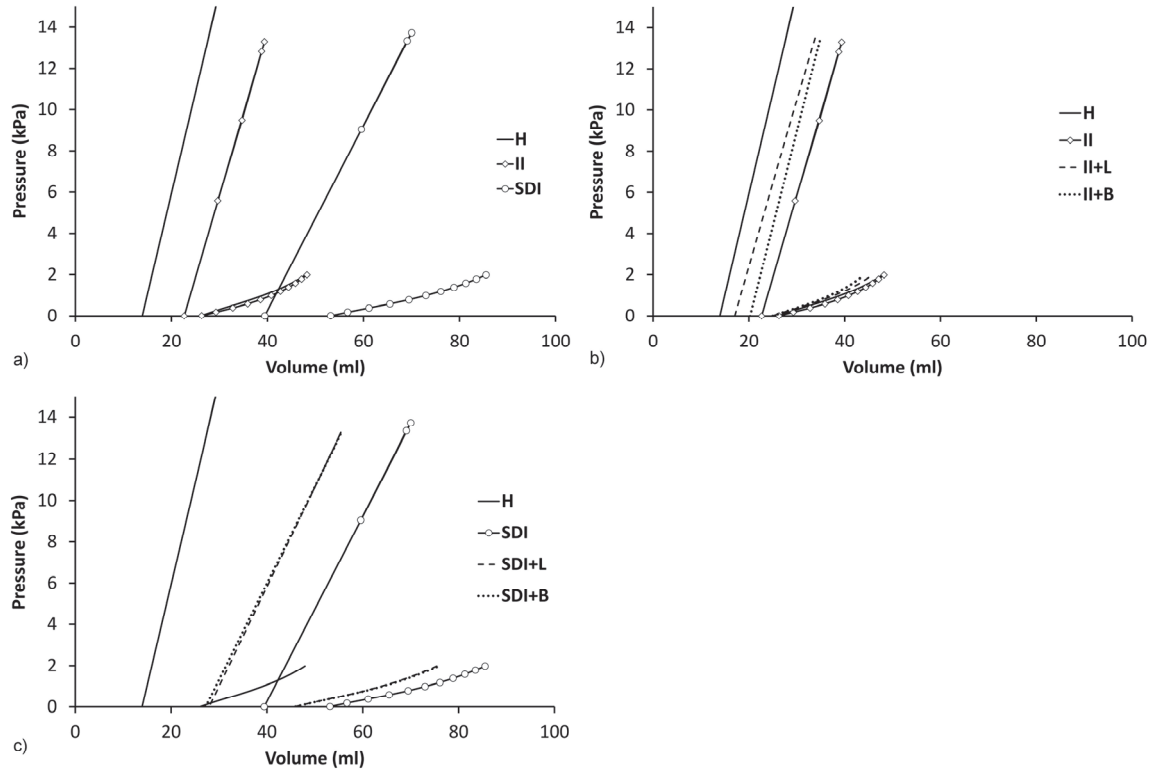


Fig. 2 Pressure-volume relationships of a) healthy (H), ischemic infarct (II) and scarred dilated infarct (SDI) models without hydrogel inclusions, b) ischemic infarct, ischemic infarct models with layered (II+L) and bulk (II+B) biomaterial inclusions, and healthy reference model, c) scarred dilated infarct, scarred dilated infarct models with layered (SDI+L) and bulk (SDI+B) biomaterial inclusions, and healthy reference mode.

### 3.1.2 Hydrogel injectates

The effect of both the layered and bulk hydrogel inclusions in the infarct on the PV relationships of the ischemic (II) and scarred dilated (SDI) infarct models is shown in Fig. 2b and c. In general, a leftward shift of the ESPVR and EDPVR curves towards the healthy control is observed due to the biomaterial incorporation in the myocardial LV wall for both hydrogel distribution and at both infarct stages. The leftward displacement of the ESPVR curves is associated with a decrease in the dead space volume,  $V_0$ . In comparison to the infarct models, improvement of cardiac contractility of 1.5% in model II+L and 7.6% in model SDI+L is shown due to layered hydrogel incorporation whereas contractility increased by 16% and 4.2% in models II+B and SDI+B, respectively, due to the bulk hydrogel injectate.

The presence of hydrogel injectate in the myocardial wall results in a decrease in  $V_0$  by 25% and 29% in models II+L and SDI+L with layered gel and by 11% and 31% in models II+B and SDI+B with bulk gel. Stroke volume increased by 65% and 40% in the layered hydrogel models II+L and SDI+L, respectively, and by 13% and 42% in bulk hydrogel models II+B and SDI+B,

respectively. The ejection fraction increased by 77% and 61% in models II+L and SDI+L, respectively, with inclusion of the layered gel, while EF increases of 25% and 63% is observed in models II+B and SDI+B, respectively, for the bulk biomaterial injectate, all compared to the respective infarct model without injectate (Table 2).

### 3.2 Myocardial mechanics

Myofibre stresses were calculated at the end-diastolic (ED) and end-systolic (ES) time points in the different cardiac models in the AA region of the infarct. The ES mid-wall myofibre stresses in the LV of the two infarct models and the healthy reference model are represented in Fig. 3. Figure 4 illustrates the mean ED and ES myofibre stresses and strains in the infarct region of the infarct models and the corresponding region of the healthy reference model.

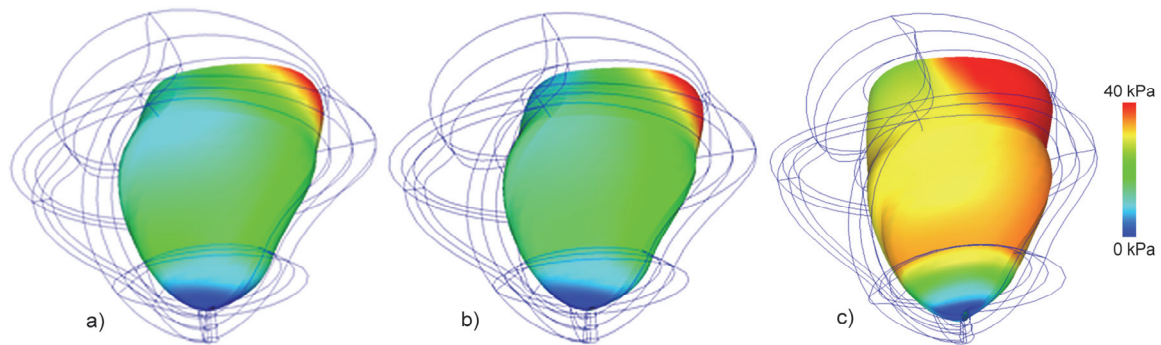


Fig. 3 Contour plot of end-systolic mid-wall myofibre stress in a) healthy LV, b) ischemic infarct model, and c) scarred dilated infarct model without hydrogel inclusions. In each plot, the wire frame depicts the contours of the biventricular cardiac geometry and the solid colour mesh indicates the mid-wall surface of the left ventricle. A frontal view of the AA region of the heart is given for each cardiac model.

#### 3.2.1 Infarct models

A general rise in ES mid-wall myofibre stresses is seen in the infarct models compared to the healthy control. The mid-wall myofibre stresses in the ischemic infarct model are slightly higher than in the healthy model. The highest ES mid-wall myofibre stresses are found in the dilated scar model. A similar trend is observed in the ED and ES mean infarct myofibre stresses (Fig. 4).

#### 3.2.2 Hydrogel injectates

With the presence of the layered hydrogel configuration, decreases of 58% and 48% in average ED myofibre strains (Fig. 4a) and of 55% and 55% in average ES myofibre strains (Fig. 4c) are found in models II+L and SDI+L, respectively. The same trend is observed for the ED and ES myofibre stresses; 78% and 58% decline in mean ED stresses (Fig. 4b) and 99% and 70% decrease in mean ES stresses (Fig. 4d) in the infarct region in models II+L and SDI+L, respectively.

Reductions of the average ED and ES myofibre stresses and strains are also observed for the infarct models with bulk hydrogel injectate, although smaller than those for layered injectate: Decreases of 31% and 14% in mean ED myofibre strains (Fig. 4a) and 30% and 23% in mean ES myofibre strains (Fig. 4c) in models II+B and SDI+B, respectively. A reduction of 67% and 16% is seen for the mean myofibre ED stress (Fig. 4b) and a decrease of 97% and 36% for the average ES myofibre stress (Fig. 4d) in models II+B and SDI+B, respectively.

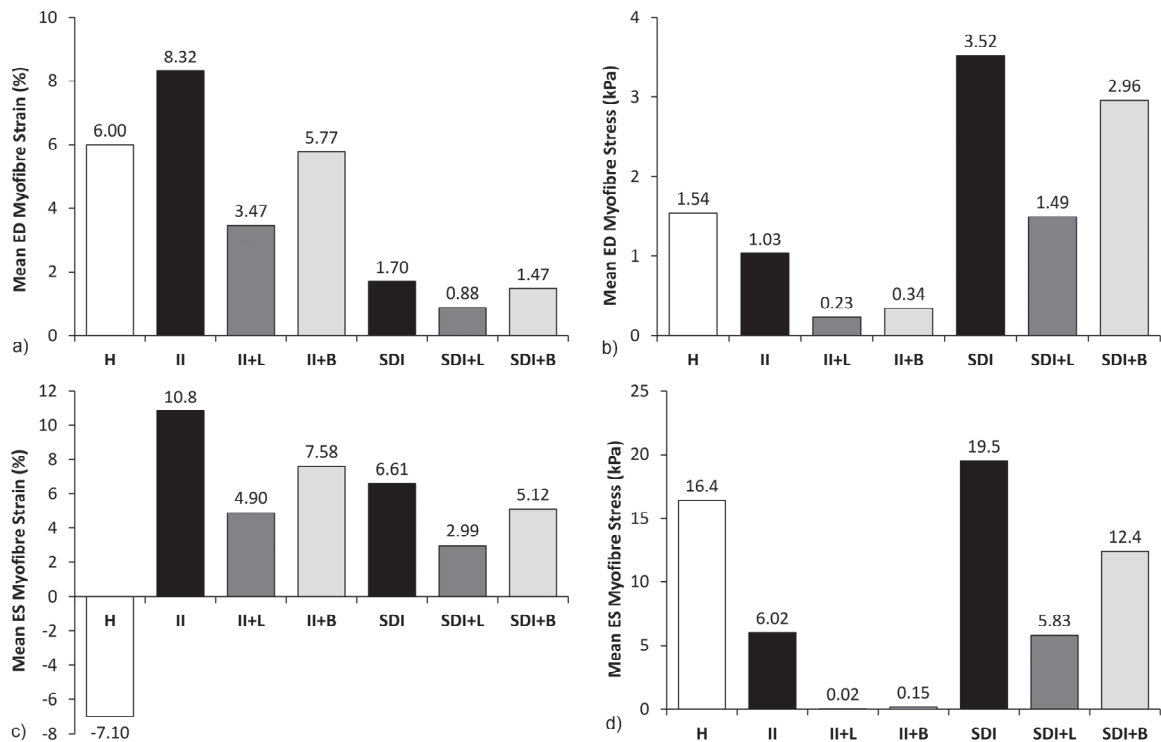


Fig. 4 Mean ED and ES myofibre stress and strain in the AA region of the heart for the healthy and infarct models with and without hydrogel layers/bulk inclusion, a) mean ED myofibre strain, b) mean ED myofibre stress, c) mean ES myofibre strain, d) mean ES myofibre stress.

#### 4. Discussion

Different approaches have been developed to prevent or limit the negative ventricular remodelling process after myocardial infarction. In one of these, biomaterial injection into the infarcted myocardial wall has shown promising results in experimental studies. To optimize and improve the outcome of this therapeutic approach, numerical studies are desirable to complement *in vivo* research. The limited number of *in silico* investigations performed on this topic so far either fashioned homogenization methods for the injectate modelling that did not consider the micro-structural distribution of the biomaterial within in the infarcted tissue (Wall *et al.* 2006, Wenk *et al.* 2011) or studied the effect of discrete biomaterial distributions in the non-infarcted LV

(Wenk *et al.* 2009). Consequently, in our previous study (Kortsmit *et al.* 2012) a layered biomaterial configuration was defined discretely, based on experimental outcomes (Dobner *et al.* 2009), and mechanical effects predicted computationally at different stages after myocardial infarction.

In the current study, the previous numerical research has been continued and successfully extended, strengthening the link to *in vivo* observations. A validated biventricular canine FE model was employed to develop models representing the presence of an antero-apical infarct in the LV at an early ischemic infarct stage and a late scarred infarct stage, the latter with a severe LV cavity dilation. Therapeutic hydrogel injectates in the infarcted region were modelled in two different configurations; layered and bulk, both based on *in vivo* studies. Functional improvement and mechanical enhancement of the infarcted LV were found after biomaterial inclusion in the infarct models. The layered hydrogel injectate seemed to be more beneficial than the bulk distribution, with regard to both cardiac function, with an exception of LV contractility, and myocardial mechanics, e.g. decreased myofibre stresses in the infarct.

#### 4.1 Cardiac function

The PV relationships and cardiac functional parameters derived for the cardiac models give a good indication of the overall LV performance.

##### 4.1.1 Effects of infarcts

It was shown that the contractility  $E_{ES}$  is smaller while the dead space volume  $V_0$ , stroke volume and ejection fraction are larger for the scarred dilated infarct model compared to the ischemic infarct case. Since the scarred infarct represents a later phase in the healing and remodelling progress that may lead to heart failure, cardiac function measures predicted with the scarred infarct model were expected to be lower than for the ischemic infarct model. The decrease in  $E_{ES}$  and increase in  $V_0$  in the dilated heart confirmed this expectation. In contrast, SV and EF were predicted to be improved in the later healing phase. However, in this stage an enlarged LV cavity has developed through increased infarct compliance and volume load in prior healing stages. The Starling mechanism preserves the SV of the LV but not the EF. The increase in the LV volume augments SV while the decrease in EF is directly related to the infarct size (Opie *et al.* 2006). This is reflected in an increase in SV by approximately 100% for the scarred dilated infarct model compared to the ischemic infarct model, whereas EF is similar for the two cases.

##### 4.1.2 Effects of hydrogel injectates

The hydrogel injectates led to an improvement of LV performance indicated by an increase in  $E_{ES}$ , SV and EV, and a reduction in  $V_0$ . Since cardiac function is affected by the mechanical properties of the myocardium, a change in mechanical properties due to hydrogel injection can lead to an improvement in ventricular performance. In both infarct models, the thickness of the infarcted wall is increased by the hydrogel incorporation, resulting in an increased overall stiffness of the LV wall. This leads to an improvement of ventricular pump function since a compliant

infarct region impairs LV contractility by tissue stretching and dissipation of energy of the healthy myocardium (Laird and Vellekoop 1977, Bogen *et al.* 1980). Whereas increased wall stiffness benefits systolic LV function, it impairs diastolic filling (Smith *et al.* 1974). This is indicated in the computational predictions by a, although small, leftward shift of the EDPVR curves after biomaterial inclusion in both infarct models. However, the results indicated the positive effect of the injectates on the systolic function outweighs the adverse effect on diastolic compliance.

For the early stage ischemic infarct, the layered injectate seemed to be more beneficial than the bulk injectate for  $V_0$ , SV and EF (Table 2) but not for cardiac contractility  $E_{ES}$ . For the scarred dilated infarct, the bulk injectate exhibited slightly more improvement than the layered injectate. A similar effect has been observed *in vivo* by Kadner *et al.* (2012) reporting a benefit of a bulk-type distribution of a hydrogel injectate, obtained with deferred biomaterial delivery, on fractional shortening that was not observed with a striated injectate distribution associated with immediate hydrogel injections.

## 4.2 Myocardial mechanics

### 4.2.1 Effects of infarcts

The ischemic and scarred infarct models in this study represent two chronological stages, early and late, after occlusion of coronary artery and of the adverse post-infarction remodelling of the heart. High stresses in the cardiac wall are known to influence the progressive structural and functional changes in the myocardium that can lead to cardiac failure (Baig *et al.* 1999). Dilation of the LV and thinning of the cardiac wall, processes part of the infarct healing and remodelling, increase the wall stress at any cavity pressure (Holmes *et al.* 2005). In the current study, this is indicated by considerable increases in stress in the infarct region of 128% and 19% (end-diastolic and end-systolic) for the scarred infarct case with stiffer and thinned infarct region and dilated LV cavity compared to the healthy LV. In contrast, stress in the infarct region in the ischemic infarct case, without cavity dilation and wall thinning, is markedly lower than in the healthy case (Fig. 4). With respect to end-diastolic myofibre strain, the ischemic infarct exhibits critical values exceeding levels reported in the healthy LV whereas the strain in the scarred infarct is far below that of the healthy AA region. Owing to lack of contractility in the infarct, mean end-systolic strain is positive, associated with stretch, in both ischemic and scarred infarct cases compared to a negative contractile strain in the healthy case.

### 4.2.2 Effects of hydrogel injectates

For strain and stress in the infarct, layered hydrogel injectates appear to perform better than bulk injectates both in the ischemic and the scarred infarct cases. Notwithstanding this difference in performance, both injectate configurations achieve a reduction of pathologically increased levels to or below values reported in the healthy LV in two instances, namely for a) end-diastolic infarct strain in the ischemic infarct case and b) end-systolic infarct stress in the scarred infarct case. However, only the layered but not the bulk injectate is able to reduce end-diastolic stress in

the scarred infarct region to physiological level. For end-systolic strain, the loss of contractility unsurprisingly dominates the infarct mechanics as the hydrogel injectates, while reducing the pathological levels, cannot establish contractile strain levels found in the corresponding healthy LV region.

#### 4.3 General cardiac modelling

The LV cavity dilation associated with post-infarct remodelling has been implemented in the cardiac models representing the late stage scarred infarct, increasing the LV cavity volume by 100% as reported by Pfeffer and Braunwald (1990) and Morita *et al.* (2011). This facilitated the consideration of the elevated wall stresses related to cavity dilation in the models and allowed the effects of the therapeutic injectates to be studied under these conditions. As such, early ischemic infarct and late scarred infarct differ not only in the constitutive properties implemented (Kortsmit *et al.* 2012) but also in ventricular configuration.

Results of pre-clinical *in vivo* studies indicated two distinctly different intra-myocardial distributions of therapeutic biomaterial injectates. Dobner *et al.* (2009) and Kadner *et al.* (2012) reported striated distributions of hyaluronic acid and PEG hydrogel, respectively, when delivered immediately after the infarct induction whereas Kadner *et al.* (2012) observed a bolus or bulk formed injectate distribution after delivery of an alginate hydrogel and PEG hydrogel, respectively, one week after the infarction. Morita *et al.* (2011) also reported a bolus like dispersion when a calcium hydroxyapatite microsphere - carboxymethylcellulose suspension was delivered immediately after infarction. It appears that the way the injectate disperses in the myocardium prior to *in situ* solidification is affected by the time point of injection after the infarct and potentially also by the injectate material. While we have simulated the layered injectate distribution before (Kortsmit *et al.* 2012), both layered and bulk injectates were modelled in the current study for comparative purposes. The discrete geometrical representation of the biomaterial injectates goes beyond the homogenized modelling of injectates (Wall *et al.* 2006, Wenk *et al.* 2011).

Compared to our previous study (Kortsmit *et al.* 2012), a different penalty function was utilized and wall stresses were calculated using the 1<sup>st</sup> instead of the 2<sup>nd</sup> Piola-Kirchhoff stress tensor. These changes, intrinsic to a later release of the cardiac modelling software Continuity employed in the current study, lead to differences in the results obtained for the same models (healthy reference and ischemic infarct). However, since 1<sup>st</sup> Piola-Kirchhoff stress tensor provides the stress relative to the reference state, i.e. the more relevant one in our case compared to the stress relative to the deformed state given by the 2<sup>nd</sup> Piola-Kirchhoff stress tensor, the current stress results were not converted although this makes the direct comparison between our two studies somewhat difficult.

## 5. Conclusions

This computational study indicated that both layered- and bulk-like intra-myocardial injectates are beneficial for improvement of cardiac function and myocardial mechanics for MI therapies. Bulk injectates showed slightly more improvement in cardiac function at late post-MI remodelling stage involving excessive dilation of the LV whereas greater benefits of the layered injectates were predicted for functional improvement at very early ischemic stage and for the reduction of stresses and strains in the infarcted cardiac wall at both ischemic and remodelled stage. With the form of the injectate distribution being associated with the time point of injection post-MI, these results may stimulate and direct further research towards tailoring this type of MI therapy.

## Acknowledgements

The authors wish to acknowledge a Claude Leon Foundation Postdoctoral Fellowship to JK and a Whitaker Foundation Fellowship to RM.

## Conflict of Interests

Conflicts of interest do not exist.

## References

- Baig, M.K., Mahon, N., McKenna, W.J., Caforio, A.L.P., Bonow, R.O. and Francis, G.S. (1999), "The pathophysiology of advanced heart failure" *Heart Lung* **28**(2), 87-101.
- Beg, M.F., Helm, P.A., McVeigh, E., Miller, M.I. and Winslow, R.L. (2004), "Computational cardiac anatomy using mri" *Magn. Reson. Med.* **52**(5), 1167-1174.
- Bogen, D.K., Rabinowitz, S.A., Needleman, A., McMahan, T.A. and Abelmann, W.H. (1980), "An analysis of the mechanical disadvantage of myocardial infarction in the canine left ventricle" *Circ. Res.* **47**(5), 728-741.
- Christman, K.L., Vardanian, A.J., Fang, Q., Sievers, R.E., Fok, H.H. and Lee, R.J. (2004), "Injectable fibrin scaffold improves cell transplant survival, reduces infarct expansion, and induces neovasculature formation in ischemic myocardium" *J. Am. Coll. Cardiol.* **44**(3), 654-660.
- Dai, W., Wold, L.E., Dow, J.S. and Kloner, R.A. (2005), "Thickening of the infarcted wall by collagen injection improves left ventricular function in rats: A novel approach to preserve cardiac function after myocardial infarction" *J. Am. Coll. Cardiol.* **46**(4), 714-719.
- Dang, A.B.C., Guccione, J.M., Mishell, J.M., Zhang, P., Wallace, A.W., Gorman, R.C., Gorman, J.H. and Ratcliffe, M.B. (2004), "Akinetic segments of myocardial infarction contain contracting. Myocytes: A finite element model study" *J. Am. Coll. Cardiol.* **43**(5), 177a.
- Dang, A.B.C., Guccione, J.M., Mishell, J.M., Zhang, P., Wallace, A.W., Gorman, R.C., Gorman, J.H. and Ratcliffe, M.B. (2005), "Akinetic myocardial infarcts must contain contracting myocytes: Finite-element model study" *Am J Physiol-Heart C* **288**(4), H1844-H1850.

- Dobner, S., Bezuidenhout, D., Govender, P., Zilla, P. and Davies, N. (2009), "A synthetic non-degradable polyethylene glycol hydrogel retards adverse post-infarct left ventricular remodeling" *J. Card. Fail.* **15**(7), 629-636.
- Doll, S. and Schweizerhof, K. (2000), "On the development of volumetric strain energy functions" *Journal of Applied Mechanics-Transactions of the Asme* **67**(1), 17-21.
- Guccione, J.M. and McCulloch, A.D. (1993), "Mechanics of active contraction in cardiac-muscle .1. Constitutive relations for fiber stress that describe deactivation" *J. Biomech. Eng.* **115**(1), 72-81.
- Guccione, J.M., McCulloch, A.D. and Waldman, L.K. (1991), "Passive material properties of intact ventricular myocardium determined from a cylindrical model" *J. Biomech. Eng.* **113**(1), 42-55.
- Guccione, J.M., Moonly, S.M., Moustakidis, P., Costa, K.D., Moulton, M.J., Ratcliffe, M.B. and Pasque, M.K. (2001), "Mechanism underlying mechanical dysfunction in the border zone of left ventricular aneurysm: A finite element model study" *Ann. Thorac. Surg.* **71**(2), 654-662.
- Holmes, J.W., Borg, T.K. and Covell, J.W. (2005), "Structure and mechanics of healing myocardial infarcts" *Annu Rev Biomed Eng* **7**(-), 223-253.
- Ifkovits, J.L., Tous, E., Minakawa, M., Morita, M., Robb, J.D., Koomalsingh, K.J., Gorman, J.H., Gorman, R.C. and Burdick, J.A. (2010), "Injectable hydrogel properties influence infarct expansion and extent of postinfarction left ventricular remodeling in an ovine model" *P Natl Acad Sci USA* **107**(25), 11507-11512.
- Kadner, K., Dobner, S., Franz, T., Bezuidenhout, D., Sirry, M.S., Zilla, P. and Davies, N.H. (2012), "The beneficial effects of deferred delivery on the efficiency of hydrogel therapy post myocardial infarction" *Biomaterials* **33**(7), 2060-2066.
- Katz, A.M. (2008), "The "modern" view of heart failure: How did we get here?" *Circ. Heart Fail.* **1**(1), 63-71.
- Kerckhoffs, R., Neal, M., Gu, Q., Bassingthwaight, J., Omens, J. and McCulloch, A. (2007), "Coupling of a 3D finite element model of cardiac ventricular mechanics to lumped systems models of the systemic and pulmonic circulation" *Ann. Biomed. Eng.* **35**(1), 1-18.
- Kortsmit, J., Davies, N.H., Miller, R., Macadangang, J.R., Zilla, P. and Franz, T. (2012), "The effect of hydrogel injection on cardiac function and myocardial mechanics in a computational post-infarction model" *Comput. Methods Biomech. Biomed. Engin.* **e-pub**(-), -.
- Laird, J.D. and Vellekoop, H.P. (1977), "The course of passive elasticity of myocardial tissue following experimental infarction in rabbits and its relation to mechanical dysfunction" *Circ. Res.* **41**(5), 715-721.
- Landa, N., Miller, L., Feinberg, M.S., Holbova, R., Shachar, M., Freeman, I., Cohen, S. and Leor, J. (2008), "Effect of injectable alginate implant on cardiac remodeling and function after recent and old infarcts in rat" *Circulation* **117**(11), 1388-1396.
- Mendis, S., Puska, P. and Norrving, B. (2011), *Global atlas on cardiovascular disease prevention and control: Policies, strategies and interventions*. World Health Organisation, Geneva.
- Morita, M., Eckert, C.E., Matsuzaki, K., Noma, M., Ryan, L.P., Burdick, J.A., Jackson, B.M., Gorman Iii, J.H., Sacks, M.S. and Gorman, R.C. (2011), "Modification of infarct material properties limits adverse ventricular remodeling" *Ann. Thorac. Surg.* **92**(2), 617-624.
- Moustakidis, P., Maniar, H.S., Cupps, B.P., Absi, T., Zheng, J., Guccione, J.M., Sundt, T.M. and Pasque, M.K. (2002), "Altered left ventricular geometry changes the border zone temporal distribution of stress in an experimental model of left ventricular aneurysm: A finite element model study" *Circulation* **106**(13 Supplement), I-168-175.
- Nelson, D.M., Ma, Z., Fujimoto, K.L., Hashizume, R. and Wagner, W.R. (2011), "Intra-myocardial biomaterial injection therapy in the treatment of heart failure: Materials, outcomes and challenges" *Acta Biomater.* **7**(1), 1-15.
- Nielsen, P.M., Le Grice, I.J., Smail, B.H. and Hunter, P.J. (1991), "Mathematical model of geometry and fibrous structure of the heart" *Am. J. Physiol. Heart Circ. Physiol.* **260**(4), H1365-H1378.
- Opie, L.H., Commerford, P.J., Gersh, B.J. and Pfeffer, M.A. (2006), "Controversies in ventricular remodelling" *Lancet* **367**(9507), 356-367.

- Pfeffer, M. and Braunwald, E. (1990), "Ventricular remodeling after myocardial infarction. Experimental observations and clinical implications" *Circulation* **81**(4), 1161-1172.
- Pilla, J.J., Gorman III, J.H. and Gorman, R.C. (2009), "Theoretic impact of infarct compliance on left ventricular function" *Ann. Thorac. Surg.* **87**(3), 803-810.
- Sam, F., Sawyer, D.B., Chang, D.L., Eberli, F.R., Ngoy, S., Jain, M., Amin, J., Apstein, C.S. and Colucci, W.S. (2000), "Progressive left ventricular remodeling and apoptosis late after myocardial infarction in mouse heart" *Am. J. Physiol. Heart Circ. Physiol.* **279**(1), H422-428.
- Smith, M., Russell, R.O., Jr., Feild, B.J. and Rackley, C.E. (1974), "Left ventricular compliance and abnormally contracting segments in postmyocardial infarction patients" *Chest* **65**(4), 368-378.
- Sun, K., Stander, N., Jhun, C.S., Zhang, Z.H., Suzuki, T., Wang, G.Y., Saeed, M., Wallace, A.W., Tseng, E.E., Baker, A.J., Saloner, D., Einstein, D.R., Ratcliffe, M.B. and Guccione, J.M. (2009), "A computationally efficient formal optimization of regional myocardial contractility in a sheep with left ventricular aneurysm" *J. Biomech. Eng.* **131**(11), 111001.
- Sutton, M.G. and Sharpe, N. (2000), "Left ventricular remodeling after myocardial infarction: Pathophysiology and therapy" *Circulation* **101**(25), 2981-2988.
- Tous, E., Ifkovits, J.L., Koomalsingh, K.J., Shuto, T., Soeda, T., Kondo, N., Gorman, J.H., 3rd, Gorman, R.C. and Burdick, J.A. (2011), "Influence of injectable hyaluronic acid hydrogel degradation behavior on infarction-induced ventricular remodeling" *Biomacromolecules* **12**(11), 4127-4135.
- Walker, J.C., Ratcliffe, M.B., Zhang, P., Wallace, A.W., Fata, B., Hsu, E.W., Saloner, D. and Guccione, J.M. (2005), "Mri-based finite-element analysis of left ventricular aneurysm" *Am. J. Physiol. Heart Circ. Physiol.* **289**(2), H692-700.
- Wall, S.T., Walker, J.C., Healy, K.E., Ratcliffe, M.B. and Guccione, J.M. (2006), "Theoretical impact of the injection of material into the myocardium: A finite element model simulation" *Circulation* **114**(24), 2627-2635.
- Wenk, J.F., Eslami, P., Zhang, Z., Xu, C., Kuhl, E., Gorman Iii, J.H., Robb, J.D., Ratcliffe, M.B., Gorman, R.C. and Guccione, J.M. (2011), "A novel method for quantifying the in-vivo mechanical effect of material injected into a myocardial infarction" *Ann. Thorac. Surg.* **92**(3), 935-941.
- Wenk, J.F., Wall, S.T., Peterson, R.C., Helgerson, S.L., Sabbah, H.N., Burger, M., Stander, N., Ratcliffe, M.B. and Guccione, J.M. (2009), "A method for automatically optimizing medical devices for treating heart failure: Designing polymeric injection patterns" *J. Biomech. Eng.* **131**(12), 121011.